Relativistic many-body calculations of excited-state energies and transition wavelengths for six-valence-electron sulfurlike ions

Yasuyuki Ishikawa*
Department of Chemistry and the Chemical Physics Program, University of Puerto Rico, P.O. Box 23346, San Juan, Puerto Rico 00931-3346, USA

Marius J. Vilkas
College of Pharmacy, University of Kentucky, 725 Rose Street, Lexington, Kentucky 40508, USA
(Received 15 August 2008; published 1 October 2008)

Relativistic multireference many-body perturbation theory calculations have been performed on sulfurlike ions as benchmarks for high-accuracy treatment of multiple open-shell ions with as many as six valence shell electrons. Term energies of the 46 excited states arising from the $3s^23p^4$, $3s3p^5$, and $3s^23p^33d$ configurations in ions of the sulfur isoelectronic sequence (Z=26–32) are evaluated to high accuracy. Transition wavelengths associated with electric dipole radiative decays were calculated with an accuracy on the order of 0.01 Å and compared with high-resolution laboratory and solar wavelength measurements to critically evaluate the line identifications.

DOI: 10.1103/PhysRevA.78.042501 PACS number(s): 31.15.am, 31.15.vj

I. INTRODUCTION

The vacuum ultraviolet (vuv) and extreme ultraviolet (euv) spectra of highly charged multi-valence-electron ions of mid-Z elements, including iron, nickel, and silicon, are observed in solar corona and cosmic sources such as late-type stars [1–6]. The complex spectra of these highly charged ions with multiple valence electrons are the signatures of events in solar corona, solar flares, and deep-space astrophysics. They have also been created in laboratory astrophysics studies using an electron beam ion trap (EBIT) to characterize them [7–10]. Fe X (Cl-like) and Fe XI (S-like) emission lines are prominent in the solar corona since iron is predominantly in the 9+ and 10+ charge states at typical coronal temperatures [6].

Although a great deal of effort has been expended during the past decades, knowledge still is fragmentary of the excited levels in sulfurlike ions of iron group elements such as Fe, Ni, and Co and their decays, which give rise to the observed euv emission spectra of multi-valence-electron systems [3,11–13]. The strongly correlated sulfurlike ions exhibit the near degeneracy characteristic of a manifold of strongly interacting configurations stemming from multiple open shells with as many as six valence electrons. Many emission lines remain unidentified because the excited levels arising from the $3s3p^5$ and $3s^23p^33d$ nominal configurations of these ions are poorly characterized [12,13]. The identifications of even some of the strongest Fe XI lines remain uncertain [14]. Of the total of 42 term energies arising from these configurations in Co XII and Ni XIII, only four have been characterized. The energy levels that experimental data are being compared to usually have been computed by semiempirical methods [15] of limited predictive power and accuracy, and this can be a source of ambiguity or misinterpretation. The paucity of well-characterized emission lines thus relates to the fact that few of the low-lying excited states have been computed using *ab initio* methods. Predicted spectral lines often have insufficient accuracy even when based on large-scale *ab initio* multiconfiguration Dirac-Fock self-consistent field (MCDF SCF) calculations [6], because the quantum mechanical underpinnings of strongly correlated systems are tremendously complicated. Since the interpretation of these spectra is severely limited by the accuracy of many-body calculations, a higher level of theory capable of providing accurate term energies must be brought to bear on atomic spectra in order to identify hitherto unidentified laboratory and solar spectral lines and to critically evaluate experimental line identifications. Such a high level of accuracy is also needed to study finer atomic properties such as parity nonconserving effects [16] and possible variation of fundamental constants [17].

Relativistic, nondynamic, and dynamic electron correlation, and quantum electrodynamic (QED) effects play a dominant role in the complex electronic structure of these ions and therefore must be accurately accounted for to correctly interpret their spectra. In a recent experimental study with the EBIT-II electron beam ion trap, Träbert, Beiersdorfer, and Chen [18] measured with unprecedented accuracy the wavelengths of the $4s_{1/2}$-$4p_{3/2}$ transitions in single-valence-electron Cu-like and two-valence-electron Zn-like ions, providing benchmarks for the theoretical underpinning of relativistic many-body theory. Their results for Cu-like ions agree very well with relativistic MCDF SCF [19] and many-body perturbation theory (MBPT) [20] calculations that include relativity, electron correlation, and QED effects. In the case of Zn-like ions, however, few extant many-body calculations provided as close an agreement with the high-resolution experiment as for the Cu-like ions. With the exception of a few multireference many-body perturbation theories [21–25], the accuracy of theoretical predictions of transition energies in two-valence-electron ions is hundredfold less accurate than for Cu-like ions [18]. The experimental study clearly indicates that theoretical predictions for

*yishikawa@uprrp.edu

two-valence-electron ions of a quality comparable to those for the one-valence-electron ions are lacking [20]. The majority of relativistic many-body methods have difficulty treating an additional electron in the valence shell [18], let alone five additional electrons in the valence shells of sulfurlike ions. The sulfurlike ions of iron group elements serve as benchmarks in the quest for a highly accurate relativistic many-body theory for truly multi-valence-electron systems.

In recent studies [24,26], we have developed an efficient procedure, in which state-averaged multiconfiguration Dirac-Fock-Breit self-consistent field (MCDFB SCF) +multireference configuration interaction (MR-CI) calculations are followed by a state-specific multireference Møller-Plesset (MR-MP) perturbation treatment, that yielded highly accurate term energies for open-shell systems with up to four valence-shell electrons. The relativistic MR-MP perturbation calculations reported for the ground and low-lying odd- and even-parity excited states of siliconlike iron demonstrated unprecedented accuracy for systems with multiple valence electrons. Highly accurate term values for all the excited states arising from the $3s^23p^2$, $3s3p^3$, $3s^23p3d$, and $3s^23p4l(l=1-3)$ configurations, including the poorly determined $3s^23p3d\ ^3F^o_{2,3,4}$ levels, were reported. In the present study, relativistic MR-MP perturbation theory calculations are performed for ions of the sulfur isoelectronic sequence $(Z=24-32)$ in order to obtain quantum mechanical underpinning of the electronic structure of strongly correlated systems involving as many as six valence-shell electrons. Transition energies of the hitherto unidentified or poorly characterized $3s3p^5$ and $3s^23p^33d$ levels of Fe XI are computed to high accuracy and compared with high-resolution laboratory and solar wavelength measurements [13,14,27,28] to critically evaluate previous level identifications.

II. COMPUTATION

The effective N-electron Hamiltonian for the development of our relativistic MR-MP algorithm is taken to be the relativistic "no-pair" Dirac-Coulomb-Breit (DCB) Hamiltonian H^+_{DCB} [29,30]. Second-order variation of the state-averaged energy $\Omega_{state\text{-}ave}$,

$$\Omega_{state-ave} = \sum_{\gamma_K \mathcal{J}\pi} \sum_{IJ}^{\mathfrak{P}(+)} C_{IK} C_{JK} \langle \Phi_I^{(+)}(\gamma_I \mathcal{J}\pi) | H^+_{DCB} | \Phi_J^{(+)}(\gamma_J \mathcal{J}\pi) \rangle \tag{1}$$

is taken with respect to the matrix elements of spinor unitary rotation matrix and configuration mixing coefficients $\{C_{IK}\}$ in the MCDFB SCF wave function,

$$\psi_K^{MC}(\gamma_K \mathcal{J}\pi) = \sum_I^{\mathfrak{P}(+)} C_{IK} \Phi_I^{(+)}(\gamma_I \mathcal{J}\pi), \tag{2}$$

leading to the Newton-Raphson equations for second-order MCDFB SCF [31]. The summation indices, γ, $\mathcal{J}$, and π, run over the ground and excited states. This state-averaged second-order MCDFB equation yields a well-balanced set of spinors suitable for describing the ground and low-lying even- and odd-parity excited $(\gamma, \mathcal{J}, \pi)$ levels. For the sulfurlike ions, the state-averaged MCDFB SCF includes a total of 48 configuration-state functions (CSF) of even and odd parity with $\mathcal{J}=0-5$, $\{\Phi_I^{(+)}(\gamma_I \mathcal{J}\pi)\}$ $(\in \mathfrak{P}^{(+)})$, arising from the $3s^23p^4$, $3s3p^5$, $3p^6$, and $3s^23p^33d$ configurations, to determine a single set of spinors for the multireference configuration interaction (MR-CI) and MR-MP calculations that follow. The key to high-accuracy algorithm for multi-valence-electron systems is the determination of a single set of spinors via the state-averaged MCDFB SCF, which provides a well-balanced description of the ground and excited levels. As the number of valence electrons n increases, the so-called V^{N-n} potential method to generate a set of spinors becomes increasingly inadequate, particularly for d and f valence electrons [32].

In order to account for strong configuration mixing among the quasidegenerate open-shell states, the MR-CI for the ground and low-lying excited $\mathcal{J}=0-5$ states in the sulfurlike ions were subsequently carried out including a total of 1,130 even- and odd-parity CSFs arising from the configurations $3s^m3p^n3d^p$, with $m+n+p=6$ and $p \leqslant 3$. Variation of the configuration-state coefficients $\{C_{IK}\}$ leads to the determinantal CI equation,

$$\det[\langle \Phi_I^{(+)}(\gamma_I \mathcal{J}\pi) | H^+_{DCB} | \Phi_J^{(+)}(\gamma_J \mathcal{J}\pi) \rangle - E^{CI} \langle \Phi_I^{(+)}(\gamma_I \mathcal{J}\pi) | \Phi_J^{(+)}(\gamma_J \mathcal{J}\pi) \rangle] = 0. \tag{3}$$

The eigenfunctions $\{\psi_K^{CI}(\gamma_K \mathcal{J}\pi)\}$ form a CI subspace $\mathfrak{P}_{CI}^{(+)}$ of the positive-energy space $\mathfrak{D}^{(+)}$,

$$\psi_K^{CI}(\gamma_K \mathcal{J}\pi) = \sum_I^{M_{CI}} C_{IK} \Phi_I^{(+)}(\gamma_I \mathcal{J}\pi), \quad K = 1,2,\ldots M_{CI}(\in \mathfrak{P}_{CI}^{(+)}). \tag{4}$$

A total of 1130 CSFs of $\mathcal{J}=0-5$, 381 even-parity and 749 odd-parity CSFs, thus produced were included in the CI calculations. The MR CI accounts for the near degeneracy in energy levels, or nondynamic correlation, inherent in multi-valence-electron systems. The frequency-dependent Breit interaction $(\Delta B(\omega))$, normal mass shift (NMS), and specific mass shift (SMS) are evaluated as the first-order corrections using the eigenvectors $\{\psi_K^{CI}(\gamma_K \mathcal{J}\pi)\}$ from the MR CI [24].

While the MR CI accounts well for the near degeneracy in energy, it fails to accurately account for dynamic correlation. Therefore, each of the 1130 CI eigenstates was subjected to state-specific MR-MP refinement to account for the residual dynamic correlation to second order of perturbation theory [26,24],

$$E_K^{(2)} = \sum_{IJ} C_{IK} C_{JK} \langle \Phi_I^{(+)}(\gamma_I \mathcal{J}\pi) | V \mathcal{R} V | \Phi_J^{(+)}(\gamma_J \mathcal{J}\pi) \rangle,$$

$$I,J = 1,2,\ldots M_{CI}(\in \mathfrak{P}_{CI}^{(+)}). \tag{5}$$

Here V is the MR-MP perturbation term, and $\mathcal{R}$ the resolvent operator acting on the subspace spanned by the residual positive-energy space $\mathfrak{Q}^{(+)}=\mathfrak{D}^{(+)}-\mathfrak{P}^{(+)}$ defined in previous study [24]. All electrons are included in the MR-MP perturbation theory calculations to determine accurately the effects of relativity on electron correlation. Radiative corrections, the Lamb shifts (LS), were estimated for each state by evalu-

TABLE I. Contributions from different orders of perturbation theory to the term energies of the ground $3s^23p^4\ ^3P_2$ and excited $3s^23p^33d^1\ ^3D_2$ states in sulfurlike ions. First-order contributions are the MR-CI energies ($E_{MR\text{-}CI}$), frequency-independent Breit interaction ($B^{(0+1)}(0)$), frequency-dependent Breit interaction ($\Delta B(\omega)$), Lamb shift (LS), normal mass shift (NMS), and specific mass shift (SMS). Next-order contributions are given by second-order Dirac-Coulomb correlation corrections ($E_{DC}^{(2)}$) and second-order Breit interaction energies ($B^{(2)}$). Energies are in atomic units.

Z	MR CI	$B^{(0+1)}(0)$	$\Delta B(\omega)$	LS	$E_{DC}^{(2)}$	$B^{(2)}$	NMS	SMS
$3s^23p^4\ ^3P_2$								
26	−1232.923158	0.463842	−0.001203	0.310895	−0.577492	−0.019312	0.012298	−0.002543
27	−1342.868876	0.526504	−0.001481	0.355182	−0.581513	−0.021038	0.012708	−0.002654
28	−1457.689157	0.594690	−0.001809	0.402403	−0.585372	−0.022843	0.013869	−0.002923
29	−1577.400432	0.668645	−0.002191	0.453816	−0.589053	−0.024731	0.013877	−0.002950
30	−1702.021059	0.748620	−0.002636	0.509620	−0.592563	−0.026702	0.014574	−0.003121
31	−1831.569488	0.834865	−0.003149	0.570022	−0.595907	−0.028756	0.014730	−0.003177
32	−1966.065853	0.927633	−0.003739	0.635228	−0.599094	−0.030897	0.015205	−0.003301
$3s^23p^33d^1\ ^3D_2$								
26	−1230.303115	0.459381	−0.001198	0.311947	−0.638799	−0.019392	0.012274	−0.002539
27	−1340.059683	0.521299	−0.001476	0.355177	−0.643990	−0.021171	0.012685	−0.002653
28	−1454.689178	0.588662	−0.001803	0.402396	−0.648911	−0.023030	0.013845	−0.002925
29	−1574.207416	0.661711	−0.002190	0.453807	−0.653556	−0.024974	0.013856	−0.002954
30	−1698.632177	0.740689	−0.002629	0.509609	−0.657938	−0.027005	0.014549	−0.003129
31	−1827.981343	0.825840	−0.003142	0.570006	−0.662066	−0.029125	0.014705	−0.003187
32	−1962.274489	0.917410	−0.003732	0.635205	−0.665944	−0.031334	0.015180	−0.003313

ating the electron self-energy and vacuum polarization following an approximation scheme discussed by Indelicato, Gorceix, and Desclaux [33]. The code described in Refs. [33,34] was adapted to our basis set expansion calculations for this purpose: All the necessary radial integrals were evaluated analytically. In this ratio method [34], the screening of the self-energy is estimated by integrating the charge density of a spinor to a short distance from the origin, typically 0.3 Compton wavelength. The ratio of the integral computed with an MCDFB SCF spinor and that obtained from the corresponding hydrogenic spinor is used to scale the self-energy correction for a bare nuclear charge as computed by Mohr [35].

The large and small radial components of the Dirac spinors are expanded in sets of even-tempered Gaussian-type functions (GTF) [36] that satisfy the boundary conditions associated with the finite nucleus [37]. The speed of light is taken to be 137.035 9895 a.u. throughout this study. The GTFs that satisfy the boundary conditions associated with the finite nucleus are automatically kinetically balanced [37]. Even-tempered basis sets of $26s24p20d$ G spinors (G for "Gaussian") for up to angular momentum $L=2$, 18 G spinors for $L=3$, and 15 G spinors for $L=4-11$ are employed. The order of the partial-wave expansion L_{max}, the highest angular momentum of the spinors included in the virtual space, is $L_{max}=11$ throughout this study. MR-MP correlation energy contributions to transition energies from partial wave $L=12$ and higher are on the order of 10 cm^{-1}. The residual correlation contributions are negligibly small for $n=3$ intrashell transitions. The nuclei were simulated as spheres of uniform proton charge with the radii $R(bohr)=2.2677\times10^{-5}A^{1/3}$, where A is atomic mass (amu).

III. RESULTS AND DISCUSSION

A. Term energies of $n=3$ levels

We illustrate our calculations on the ground $3s^23p^4\ ^3P_2$ and excited $3s^23p^33d\ ^3D_2^o$ states of sulfurlike ions with $Z=26-32$ in Table I. The table displays energy contribution from the MR CI, $E_{MR\text{-}CI}$, along with the contribution from each order of perturbation theory for the ground and excited states. The relativistic many-body shifts $B^{(2)}(0)$ that arise from including the frequency-independent Breit interaction in the effective electron-electron interaction in the second-order MR-MP perturbation calculations are given in the seventh column.

Figure 1 displays the contribution from each order of perturbation theory to the term energies of the ground $3s^23p^4\ ^3P_2$ state as functions of nuclear charge Z. The frequency-independent Breit interaction $B^{(0+1)}(0)$ in the effective electron-electron interaction included in the MR CI, as well as the Lamb shifts, result in significant corrections to the lowest-order MR-CI energy. The second-order Dirac-Coulomb correlation energies $E_{DC}^{(2)}$, nearly constant throughout the isoelectronic sequence, are of the same magnitude as $B^{(0+1)}(0)$ and LS, but with opposite sign. The $B^{(0+1)}(0)$ and LS are two orders of magnitude larger than $\Delta B^{(1)}(w)$ and SMS at the low-Z end, and increase rapidly as Z increases. Figure 2 displays the contribution from each order of perturbation theory to the $3s^23p^4\ ^3P_2$-$3s^23p^33d\ ^3D_2^o$ transition energy in S-like ions. The figure shows the importance of $E_{DC}^{(2)}$ and $B^{(0+1)}(0)$, and to a lesser extent that of $B^{(2)}(0)$ in accurately predicting the term energy separation. The contribution of $B^{(0+1)}(0)$ and $B^{(2)}(0)$ increase rapidly as Z increases along the isoelectronic sequence. NMS, SMS, LS, and

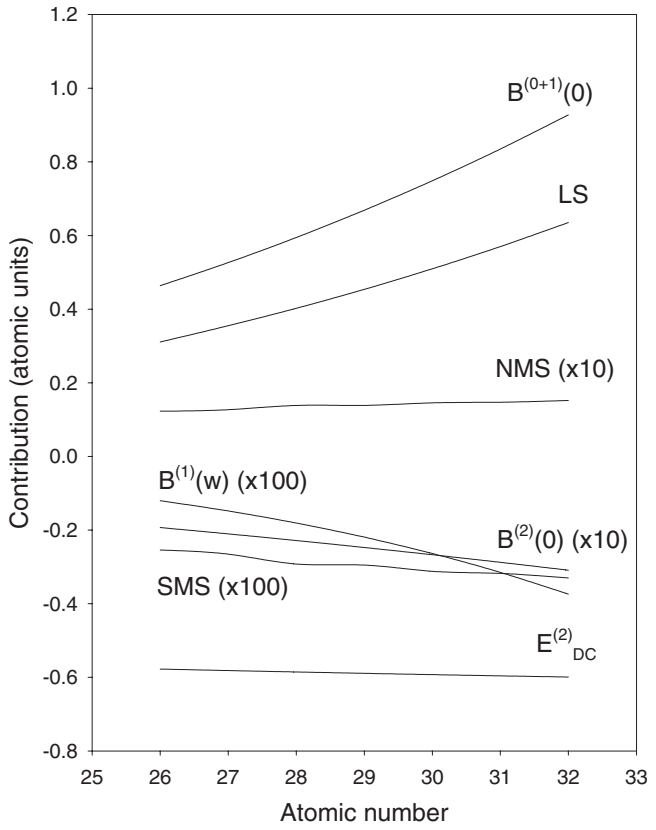

FIG. 1. Contributions from each order of perturbation theory to the term energy of the ground $3s^2 3p^4\ ^3P_2$ state in sulfurlike ions.

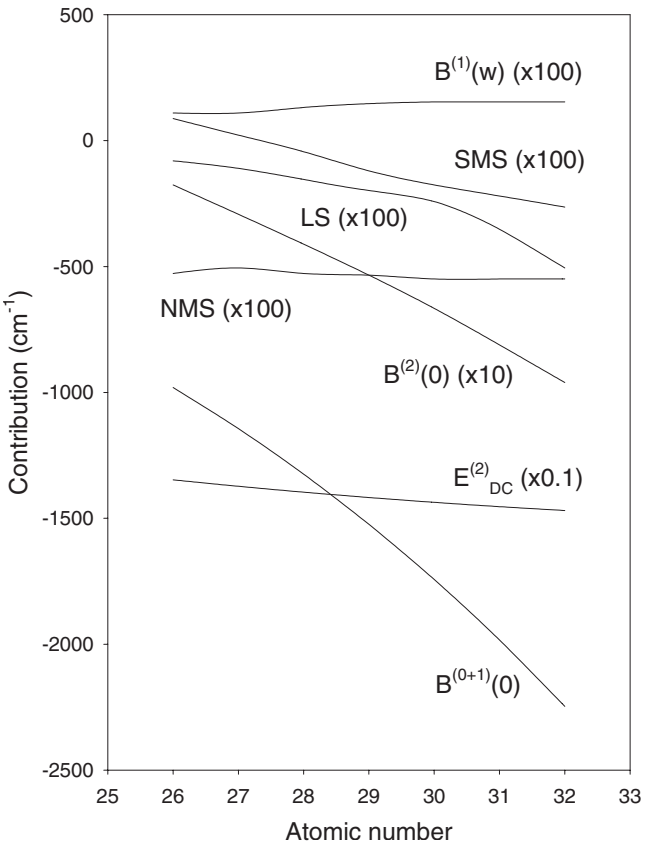

FIG. 2. Contributions from each order of perturbation theory to the $3s^2 3p^4\ ^3P_2$-$3s^2 3p^3 3d\ ^3D_2^o$ transition energy in sulfurlike ions.

$\Delta B^{(1)}(\omega)$ contribute to the term energy separation only on the order of 10 cm^{-1} through Ge XVII. The contribution of these terms to transition energies increases rapidly as Z increases [24].

Theoretical term energies of the four excited states arising from the $3s^2 3p^4$ nominal configuration are compared with available experimental data in Table II. The term energies were computed by subtracting the total energy of the ground $\mathcal{J}=2$ $(3s^2 3p^4\ ^3P_2)$ state from the total energies of the excited levels. Experimental and theoretical term energies are juxtaposed in adjacent columns under each nuclear charge Z. Experimental term energies reproduced are those compiled in the NIST Atomic Spectra Database [11]. Values in parentheses adjacent to the term energies are the percentage deviations (in hundredths of a percent) between experiment and MR-MP theory.

For the excited $3s^2 3p^4\ ^3P_{1,0}$ and $^1D_2$ levels, the theoretical term energies are in excellent agreement with experiment. Theory-experiment deviations are at the 0.01% level for all but four $^3P_0$ levels in $Z=29-32$, where the deviations range from 0.20 to 0.43 %. For the excited $^1S_0$ level in Fe^{10+} through Ge^{16+}, the deviations are in the 0.10–0.15 % range. To resolve the discrepancies for these $^3P_0$ and $^1S_0$ levels, more precise measurements are needed.

TABLE II. Comparison with experiment of MR-MP calculated term energies (cm^{-1}) of the lowest four multiplet states of sulfurlike ions arising from the $3s^2 3p^4$ configuration. Values in parentheses are the percentage deviations between theory and experiment in hundredths of a percent.

	$^3P_1$		$^3P_0$		$^1D_2$		$^1S_0$	
Z	Expt.	MR-MP	Expt.	MR-MP	Expt.	MR-MP	Expt.	MR-MP
26	12668	12665(2)	14312	14314(1)	37744	37727(5)	80815	80737(10)
27	15820	15815(3)	17070	17080(6)	42120	42106(3)	88880	88762(13)
28	19542	19535(4)	20060	20067(3)	47033	47012(4)	97836	97705(13)
29	23897	23892(2)	23192	23240(20)	52540	52520(4)	107902	107741(15)
30	28974	28959(5)	26481	26553(27)	58727	58707(3)	119210	119057(13)
31	38425	34810(941)	29860	29965(35)	65670	65656(2)	132010	131850(12)
32	41535	41522(3)	33290	33434(43)	73461	73448(2)	146478	146318(11)

Tables III and IV display the accurate term energies for all the excited levels arising from the $3s3p^5$ and $3s^23p^33d$ configurations. In the first column of the tables, the 42 odd-parity levels are each labeled according to the $\mathcal{J}$ quantum number and the order in which they appear in increasing energy. Spectroscopic term symbols are given in the second column. Of the computed 42 excited levels in Fe XI, only 21 are experimentally determined. For Co XII through Ge XVII, there are only eleven or fewer. The experimental term energies, taken from the NIST Atomic Database (NIST) and from experiments by Fritzsche *et al.* [6] and Traebert [13], are reproduced for comparison. Level numbers of the 42 states are assigned in the first column of the table. Except for the $^5D_4$ level, none of the $\mathcal{J}=4,5$ excited levels arising from the $3s^23p^33d$ configuration has been experimentally identified.

The MR-MP term energies demonstrate that theory deviates from experiment only at the 0.01% level for the hitherto available experimental term energies. Several levels in Fe XI through Ge XVII, however, display deviations up to 4.4%. The large deviations most likely arise from misidentification of the emission lines (see next section). The theoretical term energies are accurate enough that scrutiny of experimental results is warranted when deviations are 0.1% or larger. Among the excited levels that exhibit significant deviations are the Fe XI $3s^23p^33d\ ^1P_1^o$, $^3P_2^o$, Co XII $3s3p^5\ ^3P_0^o$, $3s^23p^33d\ ^1F_3^o$, Zn XV $3s3p^5\ ^3P_{2,1}^o$, and Ge XVII $3s3p^5\ ^3P_{2,1}^o$ and $3s^23p^33d\ ^3P_2^o$, $^1F_3^o$ levels, where theory deviates from experiment by as much as 0.14%–4.4%. For all these levels, theory indicates that the experimental line identifications based on semiempirical calculations are in error. In a large-scale MCDF SCF study, Fritzsche *et al.* [6] raised the question of whether the experimental $3s^23p^33d\ ^3P_2^o$ level at 496090 cm^{-1} has been correctly assigned. With as much as 0.41% theory-experiment deviation, the experimental line assignment to this level is deemed erroneous. We expect the theoretical prediction of all 42 excited levels to be accurate to the 0.01% level.

B. Transition wavelengths associated with the $E1$ radiative decays

The emission lines of Fe XI are observed in the solar spectrum under quiet conditions [38] and in the solar flare spectrum [14,28,39,40]. The energy levels of the ion have been compiled by Corliss and Sugar based on laboratory and solar spectra [41]. Wavelengths, energy levels and their classifications, and transition probabilities for the iron ions, Fe VIII–Fe XXVI, have been critically reviewed and tabulated by Shirai *et al.* [12]. Over a decade ago Jupén *et al.* [27] reported 42 new Fe X–Fe XIV lines, from which they determined a number of term energies, among them the Fe XI levels, $3s^23p^33d\ ^{1,3}P_1^o$, $^5D_{2,3}^o$, and $^3S_1^o$. In a recent study, however, Young *et al.* [14] argued that line identifications of even the strongest Fe XI lines are uncertain as the ion has a very complex atomic structure.

Table V displays the $E1$ transition probabilities and lifetimes of the energy levels of the $3s3p^5$ and $3s^23p^33d$ configurations in Fe XI. Theoretical wavelengths (λ_{theory}) of the strongest $E1$ radiative decays in the region 170–203 Å are listed in Table VI. In the table, a detailed comparison of the theoretical and experimental data is made for the transition wavelengths associated with the $E1$ radiative decay of the excited levels. Theoretical wavelengths were evaluated from the term energy separations between the upper and lower levels. Of the large number of transitions that fall in this region, only the transitions with $E1$ decay probabilities greater than $1.0\times10^{+10}$ s^{-1} are shown as they appear as strong emission lines. We expect these wavelengths to be accurate to a few hundredths of an Å. High-resolution solar line spectra obtained during the Hinode [14] mission and solar extreme ultraviolet research telescope and spectrograph (SERTS) [28] sounding rocket experiment, which have been spectroscopically assigned to the transitions in the second column, are displayed in the third (λ_{Hinode}) and fourth (λ_{SERTS}) columns. The accuracy of these solar lines is estimated at 0.01 Å. High-resolution laboratory lines with the 0.001 Å accuracy reported by Jupén, Isler, and Trabert [27] are listed in the fifth column. Observed laboratory and solar lines (in Å) compiled by Shirai *et al.* [12] are given in the last column.

Theory-experiment deviations for most of the hitherto identified lines are well within 0.1 Å, on the order of a few hundredths of an Å, underscoring the accuracy achieved by the relativistic MR-MP perturbation theory. Thus the line identification is suspect if the theory-experiment deviation approaches 0.1 Å or greater. The suspect line identifications are marked with letter "a" in the table.

Theoretical wavelength of 179.60 Å associated with the $3s^23p^4\ ^1D_2 \rightarrow 3s^23p^33d\ ^1F_3^o$ decay deviates noticeably from the experimental wavelength of 179.76 Å compiled by Shirai *et al.* This difference entails the theory-experiment percentage deviations of 0.08% in the $3s^23p^33d\ ^1F_3^o$ term energy (Table III). We ascribe the discrepancy to a line misidentification by Bromage *et al.* [42].

Theoretical wavelengths associated with decay of the $3s^23p^33d\ ^3S_1^o$ level to $3s^23p^4\ ^3P_{2,1,0}$ and $^1D_2$ levels all deviate significantly from those experimentally identified in Hinode and SERTS studies [14,28] and by Jupen *et al.* [27]. Young *et al.* [14] caution that the identification of the 188.30 Å line as the $3s^23p^33d\ ^3S_1^o$-$3s^23p^4\ ^3P_2$ transition is uncertain. We conclude that their tentative line identification is erroneous. On the other hand, the predicted wavelengths for all these transitions agree well, to within a few hundredths of an Å, with the experimentally identified lines by Bromage *et al.* [42]. As a result, the theoretical $3s^23p^33d\ ^3S_1^o$ term energy is in excellent agreement with NIST Atomic Database.

Predicted wavelengths (Å) associated with somewhat weaker $E1$ radiative decays (decay rate $\leqslant 7.0\times10^{+9}$ s^{-1}) of the excited odd-parity $3s^23p^33d$ levels to the even-parity $3s^23p^4\ ^3P_{2,1,0}$, $^1D_2$, and $^1S_0$ states in Fe XI are compared with experiment in Table VII. In the table, solar line wavelengths (λ_{Solar}) refer to the compilations by Behring [38] and by Dere [39]. The accuracy of these solar lines varies from 0.002 to 0.02 Å. Theory-experiment deviations for most of these lines are on the order of 0.01 Å.

The theoretical wavelength 202.41 Å associated with the $3s^23p^33d\ ^3P_2^o$-$3s^23p^4\ ^3P_2$ transition matches a solar line at 202.42 Å. However, this solar line has been experimentally

TABLE III. Term energies (cm^{-1}) of the odd-parity levels arising from the $3s3p^5$ and $3s^23p^33d$ configurations in ions of the sulfur isoelectronic sequence with $Z=26-29$. Values in parentheses are the percentage deviations between theory and experiment in hundredths of a percent.

		Fe^{10+}		Co^{11+}		Ni^{12+}		Cu^{13+}	
State	LS	Expt.	MR-MP	Expt.	MR-MP	Expt.	MR-MP	Expt.	MR-MP
$3s3p^5$									
2(1)	$^3P_2$	283558	283739(6)	306640	306798(5)	330215	330503(9)	354570	354881(9)
1(1)	$^3P_1$	293158	293315(5)	318280	318413(4)	344156	344412(7)		371345
0(1)	$^3P_0$	299163	299308(5)	[316430]	325938(300)		353777		382915
1(2)	$^1P_1$	361842	361675(5)	[390990]	390840(4)	420910	420846(2)	451850	451775(2)
$3s^23p^33d$									
0(2)	$^5D_0$	387760[a]	387622(4)		417606		447864		478398
0(3)	$^1S_0$		425465		458425		491767		525520
0(4)	$^3P_0$		482618		518734		555249		592258
0(5)	$^3P_0$	541720	541892(3)		582862		624665		667433
1(3)	$^5D_1$	388015[b]	387811(5)		417865		448215		478874
1(4)	$^3D_1$		417139		449739		482802		516375
1(5)	$^3D_1$		481722		516874		552117		587478
1(6)	$^3P_1$		484990		521393		558139		595298
1(7)	$^1P_1$	531070[b]	531839(14)		570625		609673		649217
1(8)	$^3S_1$	533450	533343(2)		572817		612772		653315
1(9)	$^3P_1$	541390[b]	541178(4)		582267		624174		667016
1(10)	$^3D_1$	566380	566299(1)	608660	608503(3)		651184		694431
1(11)	$^1P_1$	623080	623252(3)	[669160]	669315(2)	715960	716072(2)	763830	763720(1)
2(2)	$^5D_2$	387940[b]	388020(2)		418086		448416		478993
2(3)	$^3D_2$		412968		443891		474827		505786
2(4)	$^3F_2$		422920		455314		488158		521498
2(5)	$^1D_2$		466458		502419		538877		575876
2(6)	$^3F_2$		486227		523621		561443		599746
2(7)	$^3D_2$		489528		526933		564987		603806
2(8)	$^3P_2$	496090	494053(41)		532827		572426		612988
2(9)	$^3P_2$	531290	531502(4)	569990	570180(3)	609200	609326(2)	648960	649041(1)
2(10)	$^3D_2$	561610	561556(1)	602920	602801(2)	644660	644428(4)	686870	686531(5)
2(11)	$^1D_2$	578861	578539(6)	[622130]	621737(6)	666000	665549(7)	710770	710135(9)
3(1)	$^5D_3$	388280[b]	388335(1)		418440		448814		479362
3(2)	$^3D_3$		415477		447700		480385		513505
3(3)	$^3F_3$		426149		459062		492477		526333
3(4)	$^3G_3$		448615		482408		516423		550626
3(5)	$^3F_3$		485081		522597		560781		599614
3(6)	$^3D_3$		497452		536198		575581		615533
3(7)	$^1F_3$		525332		565991		607508		649909
3(8)	$^3D_3$	554300	554305(0)	594040	593993(1)	634000	633894(2)	674230	674043(3)
3(9)	$^1F_3$	594030	594518(8)	[630670]	638037(115)	681750	682146(6)	726770	726859(1)
4(1)	$^5D_4$	389590[c]	389274(8)		419731		450558		481705
4(2)	$^3F_4$		430589		464462		498948		533957
4(3)	$^3G_4$		450228		484605		519377		554523
4(4)	$^1G_4$		459231		494031		529192		564713
4(5)	$^3F_4$		486412		524957		564543		605173
5(1)	$^3G_5$		452413		487523		523174		559439

[a]Träbert [13].
[b]Jupén *et al.* [27].
[c]Fritzsche *et al.* (Ref. [6]).

TABLE IV. Term energies (cm^{-1}) of the odd-parity levels arising from the $3s3p^5$ and $3s^23p^33d$ configurations in ions of the sulfur isoelectronic sequence with $Z=30-32$.

		Zn^{14+}		Ga^{15+}		Ge^{16+}	
State	LS	Expt.	MR-MP	Expt.	MR-MP	Expt.	MR-MP
$3s3p^5$							
2(1)	$^3P_2$	397460	380089(437)		406109	431810	433047(29)
1(1)	$^3P_1$	398780	399351(14)		428414	457340	458613(28)
0(1)	$^3P_0$		413538		445709		479581
1(2)	$^1P_1$		483837		517078		551663
$3s^23p^33d$							
0(2)	$^5D_0$		509375		540695		572420
0(3)	$^1S_0$		559880		594793		630379
0(4)	$^3P_0$		630024		668577		708118
0(5)	$^3P_0$		711432		756745		803585
1(3)	$^5D_1$		510019		541568		573603
1(4)	$^3D_1$		550657		585606		621337
1(5)	$^3D_1$		623166		659117		695446
1(6)	$^3P_1$		633107		671566		710847
1(7)	$^1P_1$		689476		730447		772275
1(8)	$^3S_1$		694689		736906		780126
1(9)	$^3P_1$		711036		756285		802914
1(10)	$^3D_1$		738473		783321		829151
1(11)	$^1P_1$	812700	812590(1)	863000	862815(2)	915030	914664(4)
2(2)	$^5D_2$		509957		541162		572607
2(3)	$^3D_2$		536983		568373		600121
2(4)	$^3F_2$		555531		590209		625647
2(5)	$^1D_2$		613607		652022		691228
2(6)	$^3F_2$		638784		678587		719348
2(7)	$^3D_2$		643612		684389		726264
2(8)	$^3P_2$		654780		697846	743200	742328(12)
2(9)	$^3P_2$	689570	689593(0)	730990	731051(1)	773690	773684(0)
2(10)	$^3D_2$	729700	729353(5)	773220	772899(4)	817680	817334(4)
2(11)	$^1D_2$	756400	755788(8)	803320	802589(9)	851540	850762(9)
3(1)	$^5D_3$		510299		541468		572900
3(2)	$^3D_3$		547374		581942		617352
3(3)	$^3F_3$		560970		596328		632547
3(4)	$^3G_3$		585252		620212		655617
3(5)	$^3F_3$		639458		680295		722295
3(6)	$^3D_3$		656386		698076		740734
3(7)	$^1F_3$		693594		738523	782600	784636(26)
3(8)	$^3D_3$	715090	714803(4)	756600	756261(4)	799240	798896(4)
3(9)	$^1F_3$	772440	772590(2)	819360	819366(0)	867340	867401(1)
4(1)	$^5D_4$		513402		545534		578164
4(2)	$^3F_4$		569835		606498		644063
4(3)	$^3G_4$		590340		626786		664027
4(4)	$^1G_4$		600911		637767		675454
4(5)	$^3F_4$		647302		690984		736455
5(1)	$^3G_5$		596550		634505		673457

TABLE V. $E1$ transition probabilities (s^{-1}) and lifetimes (s) of the energy levels of the $3s3p^5$ and $3s^23p^33d$ configurations in Fe^{10+}.

State	LS	$^3P_2$	$^3P_1$	$^3P_0$	$^1D_2$	$^1S_0$	τ
$3s3p^5$							
2(1)	$^3P_2$	2.063(+9)	6.438(+8)		5.921(+7)		3.615(−10)
1(1)	$^3P_1$	1.338(+9)	6.954(+8)	8.855(+8)	1.819(+6)	1.251(+7)	3.409(−10)
0(1)	$^3P_0$		2.910(+9)				3.436(−10)
1(2)	$^1P_1$	2.385(+8)	1.340(+7)	5.106(+4)	7.286(+9)	2.144(+8)	1.290(−10)
$3s^23p^33d$							
0(2)	$^5D_0$		1.016(+8)				9.843(−9)
0(3)	$^1S_0$		6.426(+7)				1.556(−8)
0(4)	$^3P_0$		3.819(+8)				2.618(−9)
0(5)	$^3P_0$		1.238(+11)				8.078(−12)
1(3)	$^5D_1$	5.105(+7)	2.871(+7)	1.151(+7)	4.074(+5)	2.918(+4)	1.090(−8)
1(4)	$^3D_1$	1.646(+7)	1.537(+7)	3.052(+2)	1.429(+6)	1.900(+6)	2.844(−8)
1(5)	$^3D_1$	1.969(+8)	8.649(+7)	9.016(+8)	3.834(+8)	5.562(+7)	6.158(−10)
1(6)	$^3P_1$	2.245(+9)	2.608(+7)	9.108(+7)	2.786(+8)	4.237(+6)	3.781(−10)
1(7)	$^1P_1$	6.069(+10)	6.298(+9)	1.130(+10)	3.347(+10)	2.202(+9)	8.775(−12)
1(8)	$^3S_1$	4.132(+10)	1.168(+10)	2.800(+9)	3.649(+10)	1.456(+9)	1.067(−11)
1(9)	$^3P_1$	7.861(+8)	4.298(+10)	3.289(+10)	2.990(+10)	3.773(+9)	9.064(−12)
1(10)	$^3D_1$	2.542(+9)	5.384(+10)	7.463(+10)	2.676(+8)	3.017(+7)	7.616(−12)
1(11)	$^1P_1$	8.944(+5)	3.455(+8)	6.872(+8)	1.558(+9)	1.160(+11)	8.432(−12)
2(2)	$^5D_2$	5.701(+7)	1.153(+4)		5.488(+5)		1.737(−8)
2(3)	$^3D_2$	4.197(+7)	6.354(+6)		7.121(+6)		1.804(−8)
2(4)	$^3F_2$	1.835(+7)	7.239(+4)		8.018(+5)		5.202(−8)
2(5)	$^1D_2$	1.102(+8)	4.154(+7)		9.247(+8)		9.290(−10)
2(6)	$^3F_2$	3.159(+6)	8.634(+5)		8.452(+7)		1.129(−8)
2(7)	$^3D_2$	4.385(+8)	1.423(+9)		7.378(+7)		5.167(−10)
2(8)	$^3P_2$	4.462(+9)	9.897(+8)		1.661(+8)		1.780(−10)
2(9)	$^3P_2$	9.226(+10)	2.070(+10)		1.645(+9)		8.726(−12)
2(10)	$^3D_2$	2.829(+10)	9.936(+10)		1.784(+9)		7.726(−12)
2(11)	$^1D_2$	1.404(+8)	4.589(+9)		9.919(+10)		9.623(−12)
3(1)	$^5D_3$	2.282(+7)			3.898(+5)		4.308(−8)
3(2)	$^3D_3$	1.453(+6)			1.156(+6)		3.833(−7)
3(3)	$^3F_3$	1.060(+7)			1.016(+7)		4.817(−8)
3(4)	$^3G_3$	3.190(+7)			5.033(+7)		1.216(−8)
3(5)	$^3F_3$	1.758(+8)			6.189(+7)		4.207(−9)
3(6)	$^3D_3$	3.663(+8)			5.655(+7)		2.365(+9)
3(7)	$^1F_3$	8.976(+8)			3.249(+7)		1.075(−9)
3(8)	$^3D_3$	1.317(+11)			6.866(+7)		7.589(−12)
3(9)	$^1F_3$	2.650(+8)			1.445(+11)		6.908(−12)

identified as the intense $3s^23p^33d\ ^1P^o_1$-$3s^23p^4\ ^1D_2$ transition (see Table VI) [27,28]. Theory predicts the latter intense $3s^23p^33d\ ^1P^o_1$-$3s^23p^4\ ^1D_2$ transition at 202.38 Å, only 0.04 Å shorter than the former. Therefore, theory indicates that the less intense line associated with the $3s^23p^33d\ ^3P^o_2$-$3s^23p^4\ ^3P_2$ transition is blended with the intense $3s^23p^33d\ ^1P^o_1$-$3s^23p^4\ ^1D_2$ line. Higher-resolution observation is needed to resolve the two blended emission lines.

Theory predicts a line at 189.19 Å associated with the $3s^23p^4\ ^1D_2$-$3s^23p^33d\ ^3D^o_1$ transition, in reasonable agreement with an unclassified solar line at 189.14 ± 0.03 Å [39]. Theory also predicts a stronger line at 189.21 Å associated with the $3s^23p^4\ ^3P_1$-$3s^23p^33d\ ^3P^o_1$ transition (See Table VI). In the SERTS spectrum, Keenan *et al.* [28] identified a line at 189.19 Å as this latter transition, in excellent agreement with our theoretical prediction. Higher-resolution observation is

TABLE VI. Predicted photon wavelengths (Å) associated with strong $E1$ radiative decays of the excited odd-parity $3s^2 3p^3 3d$ levels to the even-parity $3s^2 3p^4\ ^3P_{2,1,0}$, $^1D_2$, and $^1S_0$ levels in sulfurlike Fe.

λ_{theory}	Transition	λ_{Hinode}	λ_{SERTS}	λ_{Jupen}	λ_{Shirai}
178.08	$3s^2 3p^4\ ^3P_2$-$3s^2 3p^3 3d\ ^3D^o_2$				178.06
179.60	$3s^2 3p^4\ ^1D_2$-$3s^2 3p^3 3d\ ^1F^o_3$				179.76[a]
180.41	$3s^2 3p^4\ ^3P_2$-$3s^2 3p^3 3d\ ^3D^o_3$	180.40	180.38		180.41
180.63	$3s^2 3p^4\ ^3P_1$-$3s^2 3p^3 3d\ ^3D^o_1$				180.60
181.16	$3s^2 3p^4\ ^3P_0$-$3s^2 3p^3 3d\ ^3D^o_1$		181.13		181.14
182.19	$3s^2 3p^4\ ^3P_1$-$3s^2 3p^3 3d\ ^3D^o_2$	182.16	182.17		182.17
184.33	$3s^2 3p^4\ ^1S_0$-$3s^2 3p^3 3d\ ^1P^o_1$				184.41[a]
184.91	$3s^2 3p^4\ ^1D_2$-$3s^2 3p^3 3d\ ^1D^o_2$		184.80[a]		184.80[a]
187.50	$3s^2 3p^4\ ^3P_2$-$3s^2 3p^3 3d\ ^3S^o_1$	188.30[a,b]	188.30[a]	188.306[a]	187.45
188.03	$3s^2 3p^4\ ^3P_2$-$3s^2 3p^3 3d\ ^1P^o_1$				
188.15	$3s^2 3p^4\ ^3P_2$-$3s^2 3p^3 3d\ ^3P^o_2$	188.23	188.21		188.22
188.96	$3s^2 3p^4\ ^3P_1$-$3s^2 3p^3 3d\ ^3P^o_0$		189.00		189.02
189.21	$3s^2 3p^4\ ^3P_1$-$3s^2 3p^3 3d\ ^3P^o_1$		189.19		189.13[a]
189.80	$3s^2 3p^4\ ^3P_0$-$3s^2 3p^3 3d\ ^3P^o_1$		189.72[a]		189.74
192.06	$3s^2 3p^4\ ^3P_1$-$3s^2 3p^3 3d\ ^3S^o_1$		192.88[a]		192.02
192.74	$3s^2 3p^4\ ^3P_1$-$3s^2 3p^3 3d\ ^3P^o_2$	192.83[a]	192.81[a]		192.82[a]
193.23	$3s^2 3p^4\ ^3P_0$-$3s^2 3p^3 3d\ ^1P^o_1$				
198.63	$3s^2 3p^4\ ^1D_2$-$3s^2 3p^3 3d\ ^3P^o_1$		198.56		198.55
201.77	$3s^2 3p^4\ ^1D_2$-$3s^2 3p^3 3d\ ^3S^o_1$			202.696[a]	201.74
202.38	$3s^2 3p^4\ ^1D_2$-$3s^2 3p^3 3d\ ^1P^o_1$		202.42	202.405	

[a]Suspect line identification inconsistent with data set.
[b]Tentative identification.

TABLE VII. Predicted photon wavelengths (Å) associated with weaker $E1$ radiative decays of the excited odd-parity $3s^2 3p^3 3d$ levels to the even-parity $3s^2 3p^4\ ^3P_{2,1,0}$, $^1D_2$, and $^1S_0$ states in sulfurlike Fe.

λ_{theory}	Transition	λ_{Solar}	λ_{Jupen}	λ_{Shirai}
176.59	$3s^2 3p^4\ ^3P_2$-$3s^2 3p^3 3d\ ^3D^o_1$		176.550	
176.72	$3s^2 3p^4\ ^3P_1$-$3s^2 3p^3 3d\ ^3D^o_2$			176.62[a]
184.78	$3s^2 3p^4\ ^3P_2$-$3s^2 3p^3 3d\ ^3P^o_1$		184.704[a]	
189.19	$3s^2 3p^4\ ^1D_2$-$3s^2 3p^3 3d\ ^3D^o_1$	189.14[b]		
192.61	$3s^2 3p^4\ ^3P_1$-$3s^2 3p^3 3d\ ^1P^o_1$	192.63	192.619	
192.67	$3s^2 3p^4\ ^3P_0$-$3s^2 3p^3 3d\ ^3S^o_1$	193.51[a,c]		192.64[d]
202.41	$3s^2 3p^4\ ^3P_2$-$3s^2 3p^3 3d\ ^3P^o_2$	202.42[e]		
202.52	$3s^2 3p^4\ ^1D_2$-$3s^2 3p^3 3d\ ^3P^o_2$	202.608[a]	202.600[a]	
257.51	$3s^2 3p^4\ ^3P_2$-$3s^2 3p^3 3d\ ^5D^o_3$	257.55	257.546	
257.72	$3s^2 3p^4\ ^3P_2$-$3s^2 3p^3 3d\ ^5D^o_2$	257.77	257.754	
257.86	$3s^2 3p^4\ ^3P_2$-$3s^2 3p^3 3d\ ^5D^o_1$	257.78[a]		
266.41	$3s^2 3p^4\ ^3P_1$-$3s^2 3p^3 3d\ ^5D^o_2$	266.42		
266.56	$3s^2 3p^4\ ^3P_1$-$3s^2 3p^3 3d\ ^5D^o_1$	266.60		
266.70	$3s^2 3p^4\ ^3P_1$-$3s^2 3p^3 3d\ ^5D^o_0$			

[a]Suspect line identification inconsistent with data set.
[b]Blended with the $3s^2 3p^4\ ^3P_1$-$3s^2 3p^3 3d\ ^3P^o_1$ line at 189.19 Å.
[c]SERTS observation.
[d]Blended with the $3s^2 3p^4\ ^3P_1$-$3s^2 3p^3 3d\ ^1P^o_1$ line.
[e]Alternate solar identification: Blended with the intense $3s^2 3p^4\ ^1D_2$-$3s^2 3p^3 3d\ ^1P^o_1$ line at 202.42 Å.

called for to identify the two nearly blended lines associated with the $3s^23p^4\ ^1D_2$-$3s^23p^33d\ ^3D_1^o$ and $3s^23p^4\ ^3P_1$-$3s^23p^33d\ ^3P_1^o$ transitions.

IV. CONCLUSION

Low-lying levels of sulfurlike ions of iron group elements, which feature six electrons in open valence shells that impart complex electronic structure, are poorly characterized because of the complexity of their spectra and lack of accurate theoretical predictions that guide experimental line identifications. In the present study, relativistic MR-MP calculations for the strongly correlated systems have been carried out to benchmark theoretical accuracy against high-resolution spectroscopic transitions. Transition wavelengths of the hitherto unidentified or poorly characterized excited levels of the sulfurlike ions are successfully computed with an accuracy on the order of 0.01 Å, a feat long considered difficult to achieve. Detailed comparisons are made with experiment [11–14,27,28] to critically evaluate previous level identifications.

The benchmarking places the current level of accuracy and understanding of relativistic many-body theory in the broader context in the quest for a high-accuracy many-body theory. A valuable theoretical tool for euv, vuv, and x-ray spectroscopy, the many-body theoretical method has achieved predictive capability in the spectroscopic study of strongly correlated multiple open-shell systems with as many as six valence-shell electrons.

ACKNOWLEDGMENTS

This work was supported in part by the Lawrence Livermore National Laboratory under Contract No. B568401. The authors thank Dr. E. Träbert for valuable discussions and advice on the manuscript.

[1] Chandra x-ray observatory, available at http://chandra.harvard.edu/
[2] The Solar and Heliospheric Observatory, available at http://sohowww.nascom.nasa.gov/
[3] K. P. Dere, E. Landi, H. E. Mason, B. C. Monsignori Fossi, and P. R. Young, Astron. Astrophys. Suppl. Ser. **125**, 149 (1997).
[4] E. Träbert, A. G. Calamai, G. Gwinner, E. J. Knystautas, E. H. Pinnington, and A. Wolf, J. Phys. B **36**, 1129 (2003).
[5] G. D. Sandlin, J.-D. F. Bartoe, G. E. Brueckner, R. Tousey, and M. E. VanHoosier, Ann. N.Y. Acad. Sci. **61**, 801 (1986).
[6] S. Fritzsche, C. Z. Dong, and E. Träbert, Mon. Not. R. Astron. Soc. **318**, 263 (2000).
[7] P. Beiersdorfer, Annu. Rev. Astron. Astrophys. **41**, 343 (2003).
[8] J. K. Lepson, P. Beiersdorfer, E. Behar, and S. M. Kahn, Astrophys. J. **590**, 604 (2003).
[9] J. D. Gillaspy, J. Phys. B **34**, R93 (2001).
[10] G. Brenner, J. R. Crespo López-Urrutia, Z. Harman, P. H. Mokler, and J. Ullrich, Phys. Rev. A **75**, 032504 (2007).
[11] J. R. Fuhr *et al.*, NIST Atomic Spectra Database Ver. 3.1.00, NIST Physical Reference Data, available online at http://physics.nist.gov/PhysRefDat/ASD/index.html
[12] T. Shirai, Y. Funatake, K. Mori, J. Sugar, W. L. Wiese, and Y. Nakai, J. Phys. Chem. Ref. Data **19**, 127 (1990).
[13] E. Träbert, Mon. Not. R. Astron. Soc. **297**, 399 (1998).
[14] P. R. Young, G. Del Zanna, H. E. Mason, K. P. Dere, E. Landi, M. Landini, G. A. Doschek, C. M. Brown, L. Culhane, L. K. Harra, T. Watanabe, and H. Hara, Publ. Astron. Soc. Jpn. **59**, S857 (2007).
[15] B. C. Fawcett, At. Data Nucl. Data Tables **47**, 319 (1991).
[16] V. A. Dzuba, V. V. Flambaum, and M. S. Safronova, Phys. Rev. A **73**, 022112 (2006).
[17] M. T. Murphy, J. K. Webb, and V. V. Flambaum, Mon. Not. R. Astron. Soc. **345**, 609 (2003).
[18] E. Träbert, P. Beiersdorfer, and H. Chen, Phys. Rev. A **70**, 032506 (2004).
[19] K.-T. Cheng and R. A. Wagner, Phys. Rev. A **36**, 5435 (1987).
[20] S. A. Blundell, Phys. Rev. A **47**, 1790 (1993).
[21] V. A. Dzuba, V. V. Flambaum, and M. G. Kozlov, Phys. Rev. A **54**, 3948 (1996).
[22] U. I. Safronova, W. R. Johnson, and H. G. Berry, Phys. Rev. A **61**, 052503 (2000).
[23] I. M. Savukov and W. R. Johnson, Phys. Rev. A **65**, 042503 (2002).
[24] M. J. Vilkas and Y. Ishikawa, Phys. Rev. A **72**, 032512 (2005).
[25] S. A. Blundell, W. R. Johnson, M. S. Safronova, and U. I. Safronova, Phys. Rev. A **77**, 032507 (2008).
[26] M. J. Vilkas and Y. Ishikawa, Phys. Rev. A **69**, 062503 (2004).
[27] C. Jupén, R. Isler, and E. Träbert, Mon. Not. R. Astron. Soc. **264**, 627 (1993).
[28] F. P. Keenan, K. M. Aggarwal, R. S. I. Ryans, R. O. Milligan, D. S. Bloomfield, J. W. Brosius, J. M. Davila, and R. J. Thomas, Astrophys. J. **624**, 428 (2005).
[29] J. Sucher, Phys. Rev. A **22**, 348 (1980).
[30] M. H. Mittleman, Phys. Rev. A **24**, 1167 (1981).
[31] M. J. Vilkas, Y. Ishikawa, and K. Koc, Phys. Rev. E **58**, 5096 (1998).
[32] V. A. Dzuba, Phys. Rev. A **71**, 032512 (2005).
[33] P. Indelicato, O. Gorceix, and J. P. Desclaux, J. Phys. B **20**, 651 (1987).
[34] Y.-K. Kim, in *Atomic Processes in Plasmas*, edited by Y. W. Kim and R. C. Elton, AIP Conf. Proc. No. 206 (American Institute of Physics, New York, 1990), p. 19.
[35] P. J. Mohr, Phys. Rev. A **46**, 4421 (1992).
[36] G. L. Malli, J. Da Silva, and Y. Ishikawa, Chem. Phys. Lett. **201**, 37 (1993).
[37] Y. Ishikawa, H. M. Quiney, and G. L. Malli, Phys. Rev. A **43**, 3270 (1991).
[38] W. E. Behring, L. Cohen, U. Feldman, and G. A. Doschek, Astrophys. J. **203**, 521 (1976).
[39] K. P. Dere, Astrophys. J. **221**, 1062 (1978).
[40] U. Feldman, W. E. Behring, W. Curdt, U. Schühle, K. Wilhelm, P. Lemaire, and T. M. Moran, Astrophys. J., Suppl. Ser. **113**, 195 (1997).
[41] C. Corliss and J. Sugar, J. Phys. Chem. Ref. Data **11**, 135 (1982).
[42] G. E. Bromage, R. D. Cowan, and B. C. Fawcett, Phys. Scr. **15**, 177 (1977).